Received: 26 November 2016 | Revised: 1 July 2017 | Accepted: 31 July 2017

DOI: 10.1002/jmor.20744

RESEARCH ARTICLE

WILEY JOURNAL OF morphology

Structure of supporting elements in the dorsal fin of percid fishes

Alexander F. Weickhardt | Kara L. Feilich | George V. Lauder

Department of Organismic and Evolutionary Biology, Harvard University, 26 Oxford St, Cambridge, Massachusetts 02138

Correspondence
Alexander F. Weickhardt, Museum of Comparative Zoology, 26 Oxford Street, Cambridge MA 02138.
Email: aweickhardt@alumni.harvard.edu

Funding information
This study was funded by a Harvard College Research Program grant and a Museum of Comparative Zoology Grant-In-Aid of Undergraduate Research to AW, an NSF Graduate Research Fellowship under DGE-1144152 and an MCZ Robert A. Chapman Fellowship to KF, and Office of Naval Research grant N00014-09-1-0352, monitored by Dr. Thomas McKenna to GL.

Abstract

The dorsal fin is one of the most varied swimming structures in Acanthomorpha, the spiny-finned fishes. This fin can be present as a single contiguous structure supported by bony spines and soft lepidotrichia, or it may be divided into an anterior, spiny dorsal fin and a posterior, soft dorsal fin. The freshwater fish family Percidae exhibits especially great variation in dorsal fin spacing, including fishes with separated fins of varying gap length and fishes with contiguous fins. We hypothesized that fishes with separated dorsal fins, especially those with large gaps between fins, would have stiffened fin elements at the leading edge of the soft dorsal fin to resist hydrodynamic loading during locomotion. For 10 percid species, we measured the spacing between dorsal fins and calculated the second moment of area of selected spines and lepidotrichia from museum specimens. There was no significant relationship between the spacing between dorsal fins and the second moment of area of the leading edge of the soft dorsal fin.

KEYWORDS
biomechanics, fin ray, fin spine, locomotion, second moment of area

1 | INTRODUCTION

The dorsal fin is one of the most varied swimming structures among the ray-finned fishes (Drucker & Lauder, 2001). Almost half of all fishes belong to the Acanthomorpha, a clade characterized by its spiny median fins, including the dorsal fin. In acanthomorphs, the dorsal fin is bi-partite with an anterior, spiny dorsal fin and a posterior, soft dorsal fin (Rosen, 1982). The spiny dorsal fin is supported by stiff, bony spines (Figure 1). Although there can be a few spines at the anterior edge of the soft dorsal fin, the soft fin is otherwise supported by flexible, bony rays called lepidotrichia (Figure 1). (Fin spines and lepidotrichia are hereafter referred to collectively as "fin elements.") In some acanthomorphs, the spiny and soft dorsal fins are fused into one contiguous structure. In others, a gap separates the spiny and soft dorsal fins into two discrete fins (Drucker & Lauder, 2001; Mabee, Crotwell, Bird, & Burke, 2002) (Figure 1). When there is a gap between the spiny and soft dorsal fins, the length of this gap can range from almost nothing to nearly half the length of the soft dorsal fin (Figure 1).

Although not typically the major propulsor used by swimming fishes, the dorsal fin generates important hydrodynamic forces during both steady swimming and turning (Drucker & Lauder, 2001; Tytell, 2006). For example, during steady swimming, bluegill sunfish use dorsal and anal fin undulation to produce about 50% of the thrust needed for forward propulsion (Tytell, 2006). During turning maneuvers in yellow perch, both the spiny and soft dorsal fins produce lateral and thrust forces (Tytell, Standen, & Lauder, 2007). Because the dorsal fin often generates a large proportion of a fish's propulsive forces, variation in dorsal fin morphology, including whether the spiny and soft dorsal fins are separated, likely has important consequences for hydrodynamics and overall swimming performance (Tytell, 2006).

One hydrodynamic consequence of a separated dorsal fin is that the anterior fin element of the soft fin can act as a leading edge into oncoming flow between the anterior and posterior portions of the dorsal fin. Flow visualization over a steadily swimming yellow perch, a species with a separated dorsal fin, showed that the wake generated by the anterior spiny dorsal fin collided with the leading edge of the downstream soft dorsal fin (Tytell et al., 2007).

When there is oncoming flow, stiffening a leading edge to resist flow may increase propulsive efficiency during steady swimming (Shoele & Zhu, 2012; Yates, 1983). Thus, if the spiny fin's wake adds momentum to the water encountering the soft fin, then the soft fin's leading edge may benefit from additional stiffening to resist the oncoming flow and stabilize the fin against flow-induced deformation. Given the function of the soft dorsal fin as a second leading edge in fishes with a separated dorsal fin,

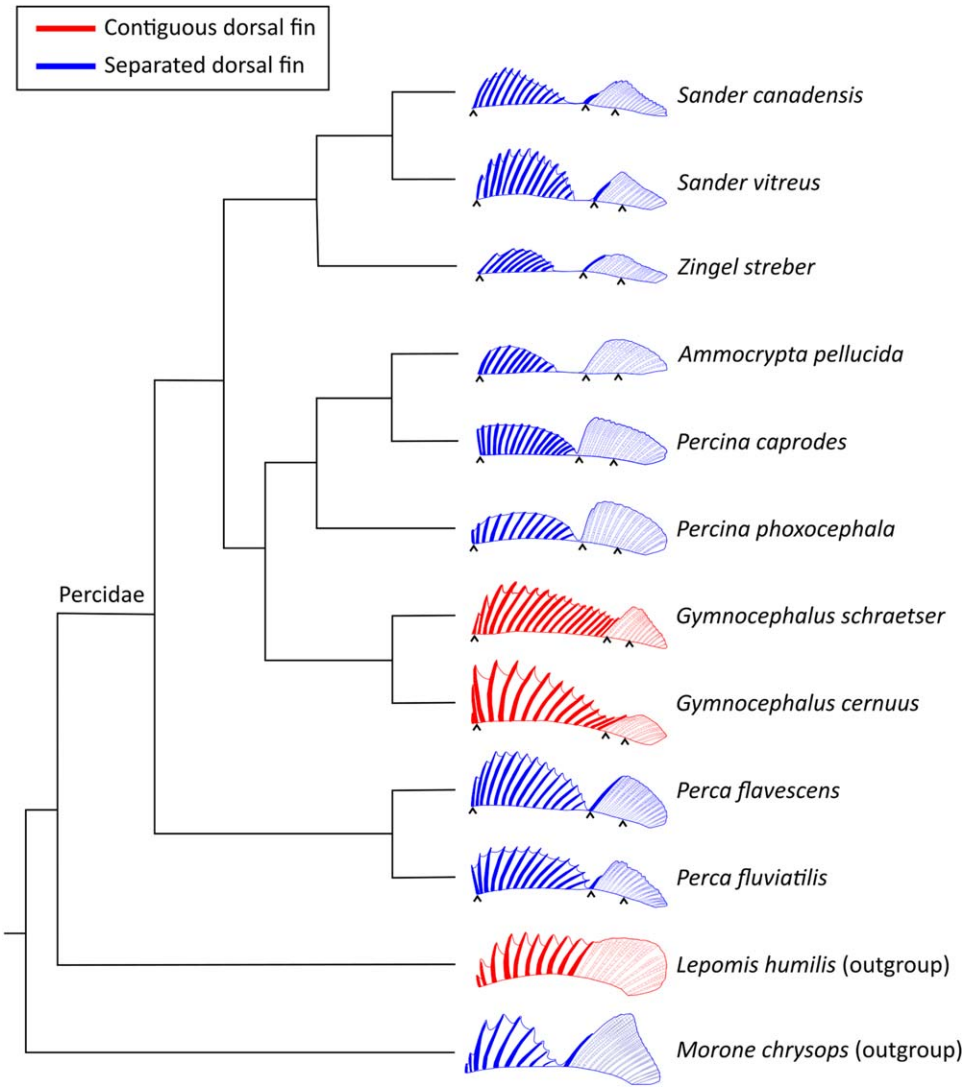

FIGURE 1 Cladogram of selected percid species (based on the phylogeny of Sloss et al., 2004) and two outgroups showing dorsal fin morphology. The dorsal fin can be present as a single contiguous structure supported by bony spines and soft lepidotrichia (red), or it may be divided into an anterior, spiny dorsal fin and a posterior, soft dorsal fin (blue). Percids exhibit great variation in dorsal fin spacing, including fishes with separated fins of varying gap length and fishes with contiguous fins. Color-filled elements indicate fin spines as opposed to lepidotrichia which are lightly shaded. The carets indicate which fin elements were examined

we predicted that the anterior of the soft fin would be stiffer in fishes with separated fins than in fishes with contiguous fins.

The development of flow between two dorsal fins depends on more than just the presence or absence of a gap between these fins. If the distance between the anterior and the posterior dorsal fin is sufficiently small, water between the two fins will move with the fins as added mass (Lighthill, 1970). As a result, there would be little or no wake shed by the spiny fin onto the soft fin. If the gap between dorsal fins is sufficiently large for flow to develop within the gap, then the posterior soft dorsal fin could function as a second leading edge (Webb & Keyes, 1981). Therefore, we hypothesized that the leading edge of the posterior soft dorsal fin would be stiffer in species with longer gaps between dorsal fins. This is admittedly an oversimplification—in fishes with extremely long gaps, the wake shed by the spiny fin would likely dissipate before it could interact with the soft fin. However, for acanthomorphs of generalist perciform body shapes, such long gaps are probably rare. Individual fin spines may also shed a wake that depends on spine shape (Maisey, 1979) and spine cross-sectional shape could generate vortices that propagate along the fin.

We studied the relationship between dorsal fin spacing and fin element structure in the family Percidae (Acanthomorpha: Percomorpha: Percidae), which includes North American and Eurasian freshwater perches (Sloss, Billington, & Burr, 2004). Percids have variation in dorsal fin spacing (Figure 1) that can be used to test the above hypotheses within a single clade.

To test the relationships between dorsal fin spacing and fin element morphology, we measured the second moment of area of three fin elements, as depicted in Figure 2: fin element 1 (FE1), the first spine of the spiny dorsal fin; fin element 2 (FE2), the first spine or lepidotrich of the soft dorsal fin and; fin element 3 (FE3), the middle lepidotrich of the soft dorsal fin (Table 1; Figure 2). Second moment of area (I) measures the contribution of both shape and size

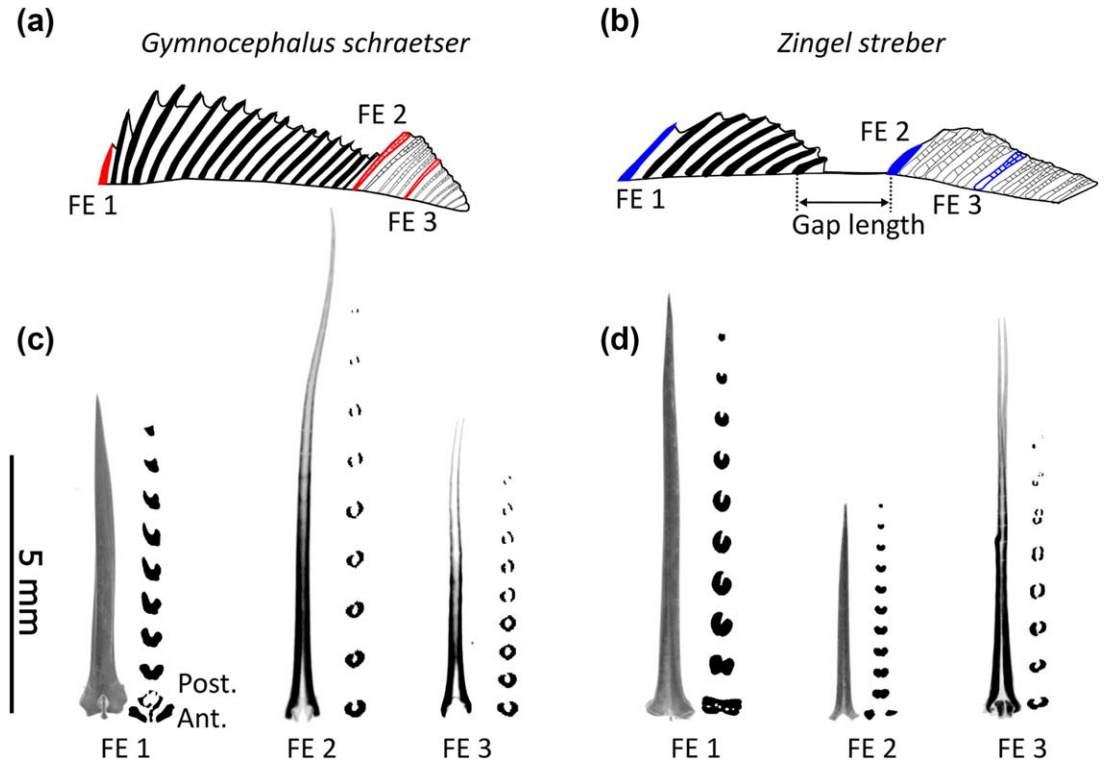

FIGURE 2 The positions of fin elements 1, 2, and 3 are indicated on drawings of both contiguous and separated dorsal fins (a, b). Gap length of a separated dorsal fin from x-ray radiographs of each individual was measured as the distance from the base of the posterior spine of the spiny fin to FE2 (b). Anterior view of micro-CT reconstructions of dorsal fin elements with binarized transaxial slices from *Gymnocephalus schraetser* (c) and *Zingel streber* (d). The third and fifth slices from the bottom are at 20% and 40% along the length of the fin elements, respectively (c, d). The darkness of the CT-images is arbitrary. The cross-sectional shapes of the fin elements varied greatly within each fin element and across different fin elements

to flexural stiffness. FE1 always serves as a hydrodynamic leading edge. Depending on the configuration of the soft and spiny dorsal fins, FE2 may also serve as a leading edge (Figure 1). Given the potential role of fin element 2 as a stiff leading edge in fishes with separated dorsal fins and the role of gap length in determining flow incipient on the soft dorsal fin, we framed the following two specific hypotheses:

I. The *I* of FE2 would increase with the length of the gap between dorsal fins as a fraction of body length to resist increased flow speeds that may develop within the gap, over the range of gap lengths observed in percids. We considered fishes with contiguous fins to have a gap length of zero.

II. As FE1 functions as a leading edge in all dorsal fin configurations, the *I* of FE1 does not depend on the spacing between dorsal fins.

We tested these hypotheses for both anteroposterior and mediolateral bending. Fin elements are not radially symmetric and flow is likely to impact the fins disproportionately along one axis of bending. As the soft dorsal fin moves, FE2 is usually at an angle to the oncoming flow (Tytell et al., 2007). As a result, the force of the water acting on the leading edge has both mediolateral and anteroposterior components with respect to that edge. Hence, both the anteroposterior and mediolateral second moments of area of fin elements at the leading edge likely affect the extent to which the leading edge is deformed by the flow it encounters.

2 | MATERIALS AND METHODS

2.1 | Specimens and fin spacing measurements

We obtained three specimens from each of ten percid species (except *Gymnocephalus schraetser*, from which we could only obtain two individuals), representing six genera. These specimens were generous loans from the ichthyology collections of the Harvard University Museum of Comparative Zoology, the National Museum of Natural History, and the University of Michigan Museum of Zoology (Supporting Information Table 1). The specimens had previously been fixed in formalin and were stored in 70% ethanol. Each specimen was radiographed. For specimens with separated dorsal fins, the space between dorsal fins was measured as the distance from the base of the posterior spine of the spiny dorsal fin to the base of FE2 (Figure 2) from the radiograph using MATLAB (v. 2015a, Natick, MA). For specimens with contiguous dorsal fins, the space between dorsal fins was counted as zero.

2.2 | Removal of fin elements and μCT imaging

FE1, FE2, and FE3 were dissected from each specimen with associated connective tissue (Figure 2). Any remaining connective tissue was carefully removed from the fin elements via fine dissection under a dissecting microscope. Each fin element was stored in 70% ethanol until use in CT-imaging. If a focal fin element was shorter than 2.5 mm, we

instead removed the fin element directly posterior to it. In these cases, the longer, posterior fin element would form a greater portion of the leading edge than the shorter anterior-most element.

To obtain cross-sectional images for the calculation of second moment of area along the length of each fin element, we micro-CT scanned each fin element using a Skyscan 1173 Micro-CT (Bruker, Billerica, MA, Hardware v. A, Software v. 1.6), with the x-ray source set at 85 kV and 80 μA. Voxel size was set between 6 and 15 μm (the highest resolution possible using this instrument) depending on the size of the focal fin element. CT-image stacks were reconstructed using NRecon (Bruker, v. 1.6.9.15). From these reconstructions, we used DataViewer (Bruker, v. 1.5.1.2) to correct for any differences in fin element alignment and create a set of transaxial image stacks depicting the cross-section of each fin element at each voxel increment along its length. These transaxial image stacks were used as the inputs for second moment of area calculations.

2.3 | Second moment of area calculation

Resistance to bending, or flexural stiffness (*EI*), of a given structure is the product of the Young's modulus (*E*), a measure of material stiffness, and the second moment of area (*I*), the contribution of size and cross-sectional shape to stiffness. *EI* can be expressed as a product of three components, to isolate the contributions of each of material properties, cross-sectional shape, and size (Table 1; Roark, Young, & Budynas, 2002):

$$EI = (E)\left(I/A^2\right)\left(A^2\right) \quad (1)$$

Where *A* is cross-sectional area.

The ratio I/A^2 is constant for a given cross-sectional shape, independent of its size (as measured by cross-sectional area). Therefore, I/A^2 serves as a shape factor reflecting how effectively a given cross-sectional shape distributes material to resist bending, independently of the total amount of material in the cross-section.

Given that all fin elements, spines and lepidotrichia alike are composed of bone, we assumed that differences in the flexural stiffness of the proximal portion of fin elements would largely result from differences in cross-sectional area and/or shape, rather than differences in material properties. Increasing either the cross-sectional area, *A*, or the shape factor, I/A^2, would increase a fin element's second moment of area, and thereby increase the flexural stiffness. If the *I* of any fin elements varied with the gap length, we sought to determine whether this trend was due to fin element shape (I/A^2), and/or fin element size (*A*).

For each transaxial image along the length of each fin element, we calculated second moment of area for both anteroposterior (I_{ap}) and mediolateral (I_{ml}) bending with a custom MATLAB program. The program first binarized the transaxial CT-image stacks using a threshold value calculated from the middle image of each stack according to Otsu's method (Otsu, 1979) (Figure 2c,d). From the binarized images, the program found the centroid of the white space in each image. We assumed that the neutral axis was a mediolateral line (for I_{ap}) or an anteroposterior line (for I_{ml}) through the centroid. Note that because the fin elements were slightly curved, the neutral axis did not necessarily pass through the centroid; however, given the high radius of curvature of the fin elements as a whole ($\gg$ 8 times the radius of the fin element cross-section) one could approximate the fin elements as straight beams with reasonable accuracy (Roark et al., 2002). The radius of curvature of the whole fin element was always at least 50 times the radius of the fin element's cross-section (Weickhardt and Feilich, personal observation), so the distances from the neutral axis to the centroid were small enough to permit use of a straight beam approximation (Roark et al., 2002). For each pixel in the binary image with a value of 1, that is, each pixel where there was bone, the program found the distance, Δy, from the pixel to the centroid-defined neutral axis. The area, *A*, of each pixel is a constant, calculated from the voxel size recorded in the CT-scan metadata for each fin element. Second moment of area is given by the equation:

$$I = \int_A (\Delta y)^2 dA \quad (2)$$

(Roark et al., 2002)

Equation 2 assumes that the beam is unbranched, but lepidotrichia have a distal branched portion. Therefore, Equation 2 may not accurately reflect the contribution of a lepidotrich's structure to its flexural stiffness along its entire length (Figure 2). However, Equation 2 may apply with acceptable accuracy to the proximal, mostly unbranched half of the lepidotrich's length. Therefore, we restricted the calculation of *I* to the proximal 40% of the lepidotrich (Figure 2). Our program calculated I_{ap} and I_{ml} using the following Riemann approximation of Equation 2 (Roark et al., 2002):

$$I \approx \sum (\Delta y_i)^2 A_i \quad (3)$$

where Δy_i is the distance of the *i*th pixel from the neutral axis and A_i is the area of one pixel.

From each binarized image along the length of each fin element, we also found the cross-sectional area, *A*, and calculated the size-independent shape factors I/A_{ap}^2 and I/A_{ml}^2 along the length of each fin element.

2.4 | Statistical analyses

To test hypotheses **(I)** and **(II),** we fit ordinary least squares regressions in MATLAB to determine the relationship between the gap length and either I_{ap} or I_{ml} (Supporting Information Tables 2 and 3; Figures 3 and 4). We fit each model with the response variable as log (*I*) for each of the three fin elements and with the predictor variables as log (body length) and gap length as a fraction of body length.

In case there was a relationship between gap length and the second moment of area of a fin element, we sought to determine whether that relationship was driven by the size or shape of the fin elements. To determine if gap length correlated with how effectively the cross-sectional shape of that fin element resisted bending, we fit a model with the response variable as I/A^2 and with the predictor variable as gap length as a fraction of body length (Supporting Information Tables 4 and 5; Supporting Information Figures 1 and 2). Similarly, to determine if the size of that fin element correlated with gap length, we fit a model with the response variable as cross-sectional area and the

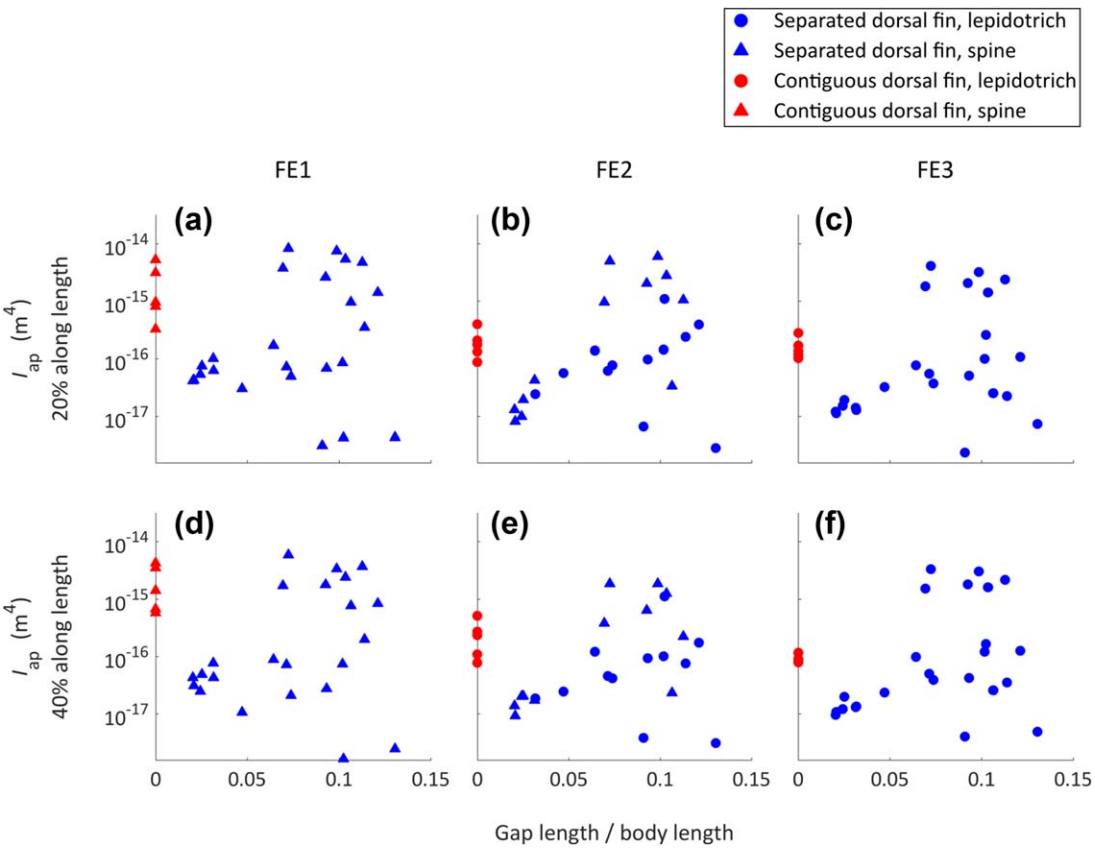

FIGURE 3 Log (second moment of area for anteroposterior bending, I_{ap}, at 20% and 40% along the length of fin elements 1, 2, and 3) plotted against gap length as a proportion of body length. Data represent eight species with separated fins and two species with contiguous fins, with two to three individuals per species. Each point corresponds to an individual fish. The axes limits are restricted to the range of the data. There was no significant correlation between I_{ap} and gap length ($p > .05$, Supporting Information Table 2)

predictor variables as both log (body length) and gap length as a fraction of body length (Supporting Information Table 6 and Supporting Information Figure 3).

While the primary goal of this study was to examine the relationship between the stiffness of fin elements and their capacity to serve as a leading edge, the data we collected also allowed us to determine the scaling relationships between body size and the cross-sectional area of the fin elements. To determine the scaling relationships between body size and the *A* of each of the three fin elements, we fit ordinary least squares regression models. Log (*A*) was the response variable and either log (body length) or log (body mass) was the predictor variable (Supporting Information Tables 7 and 8; Figures 5 and 6).

To account for the testing of multiple hypotheses, we adjusted all *p*-values using the Benjamini-Hochberg procedure. We set the false discovery rate threshold at .05 (Benjamini & Hochberg, 1995). All *p*-values mentioned hereafter are Benjamini–Hochberg adjusted.

3 | RESULTS

3.1 | No significant relationship between dorsal fin spacing and second moment of area

For all fin elements, there was no significant relationship between second moment of area and gap length as a fraction of body length ($p > .05$; Supporting Information Tables 2 and 3; Figures 3 and 4). Similarly, neither fin element cross-sectional area nor the effectiveness of the fin element shapes to resist bending correlated with gap length ($p > .05$, Supporting Information Tables 4–6, Supporting Information Figures 1–3).

3.2 | Variation in cross-sectional shape

At 20% along the length of almost every fin element, I/A_{ml}^2 was greater than I/A_{ap}^2 (Supporting Information Figures 1a–c and 2a–c). At 40% along the length of the fin elements, there was no consistent difference between I/A_{ap}^2 and I/A_{ml}^2 (Supporting Information Figs. 1d–f and 2d–f).

Additionally, the cross-sectional shape of fin elements varied across fin elements, and within individual fin elements. The cross-sections of spines ranged from dumbbell-shaped, such as in FE2 of *Z. streber*, to celery-shaped, such as in FE1 of *G. schraetser* (Figure 2c,d). The cross-sections of lepidotrichia ranged from celery-shaped, such as in the proximal part of FE2 in *G. schraetser*, to bilateral crescents, such as in the distal part of FE2 in *G. schraetser* (Figure 2c,d). Within most fin elements, the cross-section was wider proximally and narrower distally (Figure 2c,d). Some of this within fin-element variation may be due to the anatomical means by which the fin element is articulated with the supporting endoskeletal structures. Even between the two

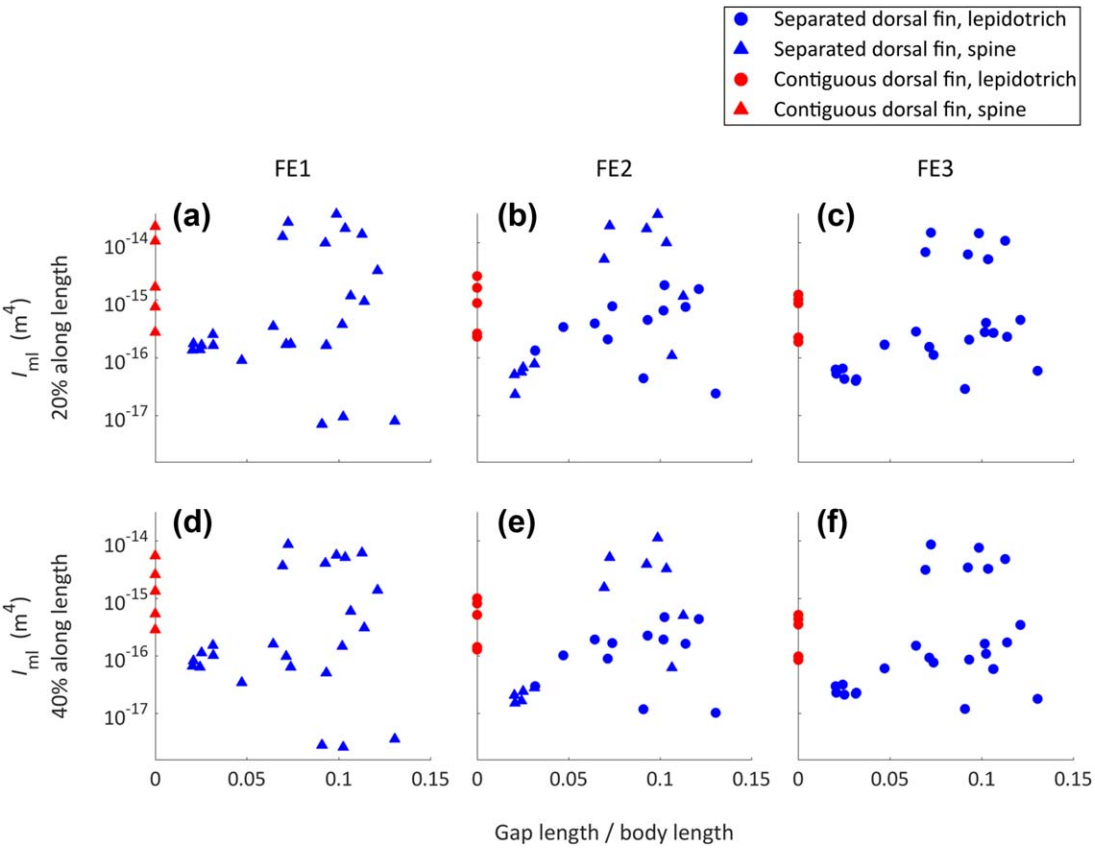

FIGURE 4 Log (second moment of area for mediolateral bending, I_{ml}, at 20% and 40% along the length of fin elements 1, 2, and 3) plotted against gap length as a proportion of body length. The data represent eight species with separated fins and two species with contiguous fins, with two to three individuals per species. Each point corresponds to an individual fish. Axis limits are restricted to the range of the data. There was no significant correlation between I_{ml} and gap length ($p > .05$, Supporting Information Table 3)

species with the most different dorsal fin element morphology observed (*G. schraetser* and *Z. streber*), the patterns of taper along the length of the fin elements were generally similar (Supporting Information Figure 4). Variance across the fin elements of any individual fish was also minimal, as evidenced by the linear relationships across fin elements (Supporting Information Figures 5 and 6). Fishes with FE1 of high cross-sectional area also had high cross-sectional area for FE2 and FE3 (Supporting Information Figure 5). Similarly, fishes with FE1 of high second moment of area also had high second moment of area for FE2 and FE3 (Supporting Information Figure 6).

3.3 | Cross-sectional area scaled against body length with negative allometry

The cross-sectional area of most fin elements showed strongly negative allometry when scaled against body length or body mass. For fish body length and *A*, isometric scaling predicted a slope of 2.0. The observed slope ranged from 0.87 to 1.59 (Figure 5). For body mass and *A*, isometric scaling predicted a slope of 0.66. The observed slope ranged from 0.24 to 0.47 (Figure 6). In all cases, except the regression of the *A* of FE3 against body mass, the slopes were significant ($p < .05$; Supporting Information Tables 7 and 8).

4 | DISCUSSION

4.1 | Relationship between dorsal fin spacing and FE2 second moment of area

In computational models of a single flexible fin similar to a soft dorsal fin, stiffening the leading edge of that fin to resist oncoming flow reduced drag and thereby raised propulsive efficiency in steady swimming (Shoele & Zhu, 2012). Unlike the fins in those models, the soft dorsal fin of a fish with a separated fin does not move in isolation, but instead moves in the wake of the upstream spiny fin (Feilich & Lauder, 2015; Tytell et al., 2007). Because FE2 is a leading edge in fishes with long gaps between dorsal fins, we predicted *I* of FE2 to be correlated with the length of the gap between dorsal fins. However, we observed no such relationship (Figures 3 and 4). This was surprising given that FE2 was often a spine in separated fins, but always a lepidotrich in contiguous fins (Figure 2). We expected that the presence of a spine at FE2 would give FE2 a greater *I* in separated fins than in contiguous fins, as spines are not completely hollow but lepidotrichia are hollow (Figure 2). However, the *I* of FE2 did not depend on whether FE2 was a spine or a lepidotrich (Figures 3 and 4).

There are three plausible explanations for the lack of a relationship between gap length and second moment of area in the species

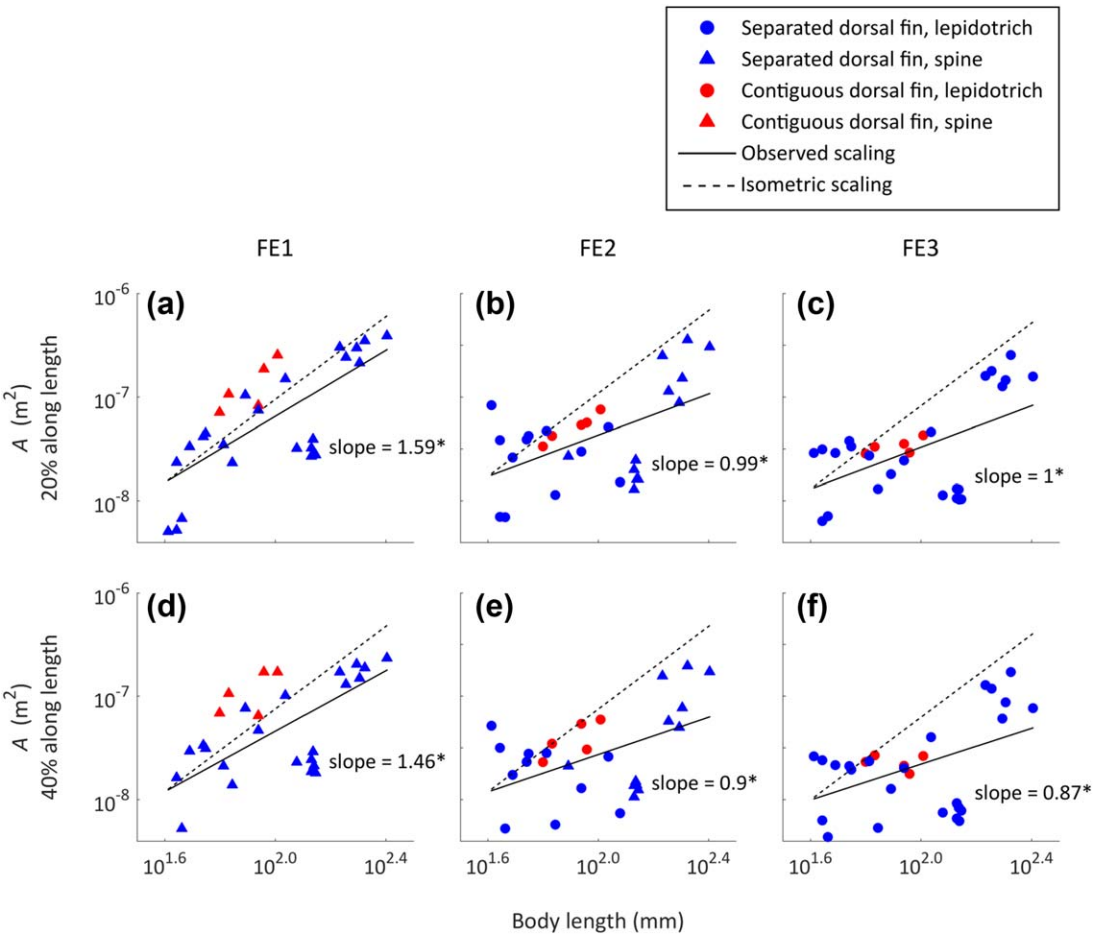

FIGURE 5 Ordinary least squares regressions of log (cross-sectional area, *A*, at 20% and 40% along the length of fin elements 1, 2, and 3) plotted against log (body length). Data represent eight species with separated fins and two species with contiguous fins, with two to three individuals per species. Each point corresponds to an individual fish. Axis limits are restricted to the range of the data. *regression coefficient with $p < .05$. The cross-sectional area of the fin elements generally scaled against body length with strongly negative allometry, especially for FE2 and FE3 (Supporting Information Table 7)

measured. (1) A stiffened leading edge on the soft portion of a separated fin does not provide any hydrodynamic benefit in steady swimming, or such a benefit is not being exploited by these fishes. (2) There is a hydrodynamic benefit in steady swimming to a stiffened leading edge on the soft portion of a separated fin, but these fishes use alternative means of stiffening the leading edge, such as activation of intrinsic fin musculature or modifying the material properties of fin elements, rather than modifying structural properties. (3) The planar area of the fins and shape of the gap are more important determinants of the hydrodynamic load on the posterior fin than is the gap length.

One possible reason for the lack of a hydrodynamic benefit to stiffening the soft fin's leading edge in these species is that either the length of the gap between the spiny and soft fins or the orientation of the two fins may preclude any potential hydrodynamic interaction. If the gap between fins is either too large or too small, the wake of the spiny fin may not interact with the leading edge of the soft fin during steady swimming. If the gap between fins were too large, the wake shed by the spiny fin would likely dissipate before it could collide with the soft fin (Drucker & Lauder, 2001). If the gap between fins were too small, the fins may behave similarly to a contiguous fin, with little or no wake shed by the spiny fin (Feilich & Lauder, 2015; Lighthill, 1970). Also, if the arrangement of dorsal fins caused the posterior fin to experience reduced flow, for example if vorticity were shed primarily laterally by the anterior fin, one would also expect no benefit from FE2 stiffening. Water flow patterns in the wake of fin surfaces that are not smooth but are interspersed with fin spines or rays are likely to be complex (Lauder et al., 2016; Maisey, 1979) and predicting forces on fins with differing gap lengths in the absence of experimental data is challenging.

Alternatively, fish may benefit from stiffening the leading edge of the soft dorsal fin, but they achieve stiffening through means other than structural modification. Fishes with separated fins may stiffen fin elements voluntarily using inclinator and/or erector muscles attached to the base of each fin element (Lauder et al., 2011). Contracting these fin muscles increases lepidotrich stiffness by more than tenfold (Alben, Madden, & Lauder, 2007). Even when FE2 is a spine, the spine could actively resist bending through contraction of the erector muscles (Chadwell, Standen, Lauder, & Ashley-Ross, 2012). If greater active stiffening of fin elements sufficiently stiffens the soft fin's leading edge

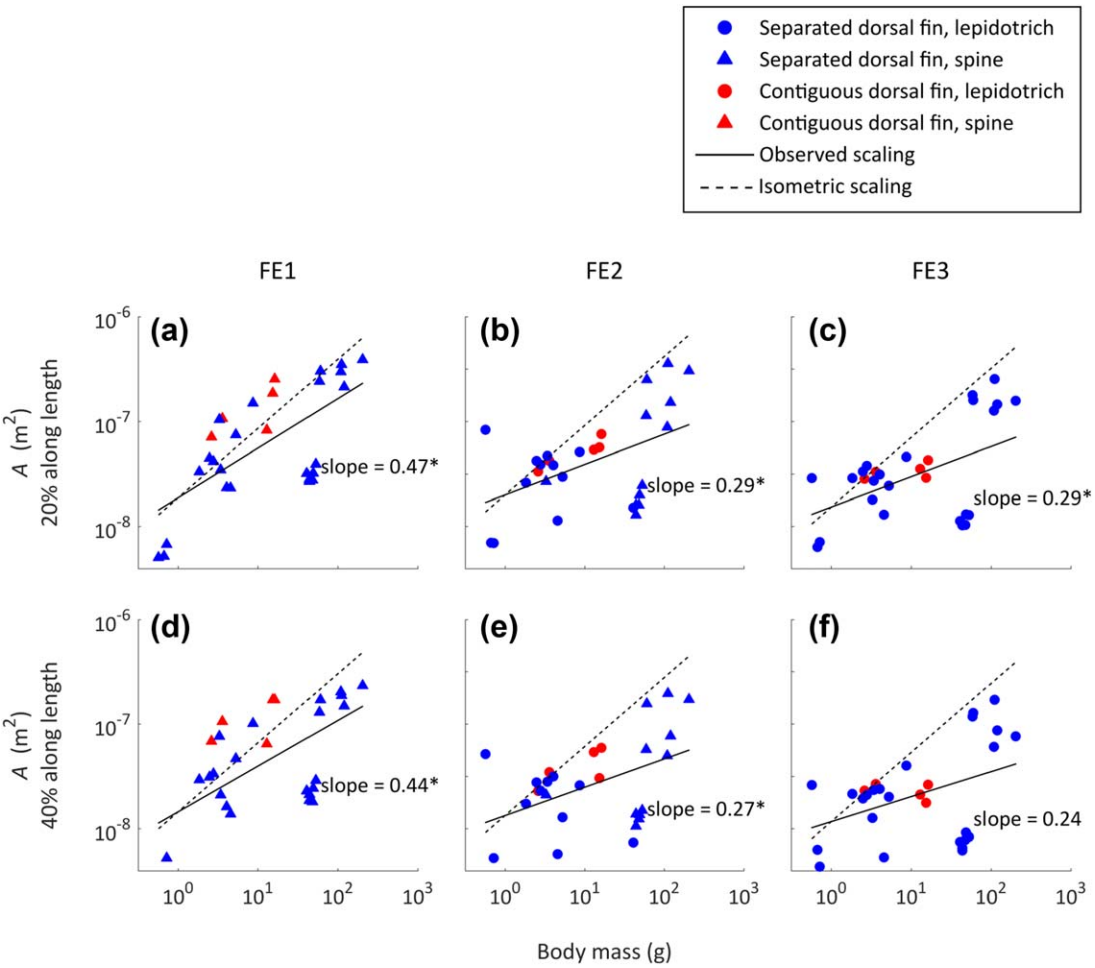

FIGURE 6 Ordinary least squares regressions of log (cross-sectional area, *A*, at 20% and 40% along the length of fin elements 1, 2, and 3) plotted against log (body mass). Data represent eight species with separated fins and two species with contiguous fins, with two to three individuals per species. Each point corresponds to an individual fish. Axis limits are restricted to the range of the data. *regression coefficient with $p < .05$. The cross-sectional area of all fin elements scaled against body mass with strongly negative allometry (Supporting Information Table 8)

to resist oncoming flow, it would be unnecessary to change the passive structural and material properties of the fin elements to reap the hydrodynamic benefits of leading edge stiffening.

TABLE 1 List of symbols and abbreviations

Symbol	Definition
FE1	Fin element 1: first element of the spiny dorsal fin (always a spine)
FE2	Fin element 2: first element of the soft dorsal fin (either a spine or lepidotrich)
FE3	Fin element 3: middle element of the soft dorsal fin (always a lepidotrich)
I_{ap}	Second moment of area, anteroposterior bending
I_{ml}	Second moment of area, mediolateral bending
A	Cross-sectional area
I/A_{ap}^2	Ratio of second moment of area to the square of cross-sectional area, anteroposterior bending
I/A_{ml}^2	Ratio of second moment of area to the square of cross-sectional area, mediolateral bending

It is also possible that the leading edge of the soft dorsal fin is stiffened by altered material properties, rather than by modified structural properties. We assumed that any correlation between gap length and the flexural stiffness of FE2 would be driven by differences in the structural properties of fin elements, as fin elements are all chiefly composed of bone. However, it is possible that the effective (composite) Young's modulus of FE2 is greater in fishes with separated fins because FE2 is often a spine in these species but always a lepidotrich in fishes with contiguous fins (Figure 2). Spines are almost entirely bone, but lepidotrichia consist of a large amount of ligament and a collagenous gel in addition to bone (Alben et al., 2007; Lauder, 2015). If spines have a greater composite Young's modulus than lepidotrichia, having a spine at the soft dorsal fin leading edge would make it unnecessary to change the structural properties of the fin elements to achieve leading edge stiffening.

Finally, the shape of the gap and the planar area of the fins may have greater effects than does the gap length on the hydrodynamic forces on the posterior fin. The shape of the gap would likely affect the wake shed by the anterior fin and consequently affect the forces on the posterior fin. Similarly, the planar area of the posterior

fin would affect the mass of fluid interacting with the fin and therefore affect the hydrodynamic forces on that fin. If the shape of the gap and planar fin area are the main determinants of the hydrodynamic load on the posterior fin, then the stiffness of FE2 would be largely determined by these two variables and not by the gap length. However, we were unable to measure accurately the planar area of the fins and shape of the gap due to the manner in which the specimens were fixed.

4.2 | Cross-sectional area and fin element allometry

The cross-sectional area of most fin elements scaled against body size with strongly negative allometry (Figures 5 and 6). Negative allometry may serve to reduce disproportionately high drag costs in larger fish. Drag is proportional to speed squared times area perpendicular to the flow. As larger fish swim at greater speeds (Bainbridge, 1958), the drag contributed by each additional unit of fin area is greater in a larger fish. The reason that larger fish have smaller fin elements relative to their body size may be to limit the area of the fin perpendicular to flow and therefore limit drag.

An alternative explanation that is not mutually exclusive of hydrodynamic explanations may be the role of fin spines as an anti-predation defense (Hoogland & Morris, 1956). Smaller fishes likely have greater need of spines as an anti-predator defense to increase size relative to a predator's gape width. As fishes grow, such defenses may not be as important. This is corroborated by previous findings demonstrating negative allometry between spines and other measurements of size by Price and colleagues, though that was not the primary purpose of their study (Price, Friedman, & Wainwright, 2015).

4.3 | Future directions

We did not find any relationship between the capacity of fin elements to function as leading edges and the stiffness of those fin elements. However, given the large reduction in drag caused by stiffening the leading edge of an otherwise flexible fin observed in computational studies (Shoele & Zhu, 2012), the stiffness of the fin elements at the leading edges of the dorsal fins may nonetheless have important effects on swimming hydrodynamics. Differences in the stiffness of pectoral fin elements between species have been shown to have important effects on the swimming function of the fin (Taft, 2011; Taft, Lauder, & Madden, 2008; Taft & Taft, 2012), so it is plausible that any variation in dorsal fin stiffness may have large effects on swimming function.

Addressing these questions will require a combination of flow visualization over dorsal fins of different configurations during swimming, estimates of drag on both first and second dorsal fins, measurements of fin area and fin shape, and study of variation in dorsal fin kinematics across species with different fin configurations. More challenging experimentally, but of great utility, would be the direct measurement of forces on spines and rays within the dorsal fin during locomotion.

ACKNOWLEDGMENTS

Many thanks to Karsten Hartel and Andrew Williston of the Harvard MCZ for their assistance in procuring specimens, and Dave Johnson of the NMNH and Douglas Nelson of the UMMZ for their generous loans. Additional thanks to Kelsey Lucas, Andrew Biewener, Stacey Combes, and Natalia Taft for helpful discussions.

CONFLICT OF INTEREST

We declare no conflict of interest.

AUTHOR CONTRIBUTIONS

AW and KF designed the study. AW conducted all imaging, programmed the MATLAB scripts for processing and analysis, and wrote the first draft of the manuscript. AW and KF analyzed and interpreted the data, and AW, KF, and GL revised the manuscript.

ORCID

Alexander F. Weickhardt http://orcid.org/0000-0002-8195-3764
Kara L. Feilich http://orcid.org/0000-0001-6057-897X
George V. Lauder http://orcid.org/0000-0003-0731-286X

REFERENCES

Alben, S., Madden, P. G., & Lauder, G. V. (2007). The mechanics of active fin-shape control in ray-finned fishes. *Journal of The Royal Society Interface*, *4*, 243–256.

Bainbridge, R. (1958). The speed of swimming of fish as related to size and to the frequency and amplitude of the tail beat. *Journal of Experimental Biology*, *35*, 109–133.

Benjamini, Y., & Hochberg, Y. (1995). Controlling the false discovery rate: A practical and powerful approach to multiple testing. *Journal of the Royal Statistical Society: Series B*, *57*, 289–300.

Chadwell, B. A., Standen, E. M., Lauder, G. V., & Ashley-Ross, M. A. (2012). Median fin function during the escape response of bluegill sunfish (*Lepomis macrochirus*). I: Fin-ray orientation and movement. *Journal of Experimental Biology*, *215*, 2869–2880.

Drucker, E. D., & Lauder, G. V. (2001). Locomotor function of the dorsal fin in teleost fishes: Experimental analysis of wake forces in sunfish. *Journal of Experimental Biology*, *204*, 2943–2958.

Feilich, K. L., & Lauder, G. V. (2015). Passive mechanical models of fish caudal fins: Effects of shape and stiffness on self-propulsion. *Bioinspiration & Biomimetics*, *10*, 036002.

Hoogland, R. D., & Morris, D. T. (1956). The spines of sticklebacks (*Gasterosteus* and *Pygosteus*) as a means of defence against predators (*Perca* and *Esox*). *Behaviour*, *10*, 205–237.

Lauder, G. V. (2015). Flexible fins and fin rays as key transformations in ray-finned fishes. In K. P. Dial, N. Shubin, & E. Brainerd (Eds.), *Great transformations in vertebrate evolution* (pp. 31–45). Berkeley, CA: University of California Press.

Lauder, G. V., Madden, P. G. A., Tangorra, J., Anderson, E., & Baker, T. V. (2011). Bioinspiration from fish for smart material design and function. *Smart Materials and Structures*, *20*, 094014.

Lauder, G. V., Wainwright, D. K., Domel, A. G., Weaver, J., Wen, L., & Bertoldi, K. (2016). Structure, biomimetics, and fluid dynamics of fish skin surfaces. *Physical Review Fluids*, *1*, 060502.

Lighthill, M. J. (1970). Aquatic animal propulsion of high hydromechanical efficiency. *Journal of Fluid Mechanics*, *44*, 265–301.

Mabee, P. M., Crotwell, P. L., Bird, N. C., & Burke, A. C. (2002). Evolution of median fin modules in the axial skeleton of fishes. *Journal of Experimental Zoology*, *294*, 77–90.

Maisey, J. (1979). Finspine morphogenesis in squalid and heterodontid sharks. *Zoological Journal of the Linnean Society*, *66*, 161–183.

Otsu, N. (1979). A threshold selection method from gray-level histograms. *IEEE Transactions on Systems, Man, and Cybernetics: Systems*, *9*, 62–66.

Price, S. A., Friedman, S. T., & Wainwright, P. C. (2015). How predation shaped fishes: The impact of fin spines on body form evolution across teleosts. *Proceedings of the Royal Society B*, *282*, 20151428.

Roark, R. J., Young, W. C., & Budynas, R. G. (2002). *Roark's formulas for stress and strain* (7th ed.). New York: McGraw-Hill.

Rosen, D. E. (1982). Teleostean interrelationships, morphological function and evolutionary inference. *American Zoologist*, *22*, 261–273.

Shoele, K., & Zhu, Q. (2012). Leading edge strengthening and the propulsion performance of flexible ray fins. *Journal of Fluid Mechanics*, *693*, 402–432.

Sloss, B. L., Billington, N., & Burr, B. M. (2004). A molecular phylogeny of the Percidae (Teleostei, Perciformes) based on mitochondrial DNA sequence. *Molecular Phylogenetics and Evolution*, *32*, 545–562.

Taft, N., Lauder, G. V., & Madden, P. G. (2008). Functional regionalization of the pectoral fin of the benthic longhorn sculpin during station holding and swimming. *Journal of Zoology*, *276*, 159–167.

Taft, N. K. (2011). Functional implications of variation in pectoral fin ray morphology between fishes with different patterns of pectoral fin use. *Journal of Morphology*, *272*, 1144–1152.

Taft, N. K., & Taft, B. N. (2012). Functional implications of morphological specializations among the pectoral fin rays of the benthic longhorn sculpin. *Journal of Experimental Biology*, *215*, 2703–2710.

Tytell, E. D. (2006). Median fin function in bluegill sunfish *Lepomis macrochirus*: Streamwise vortex structure during steady swimming. *Journal of Experimental Biology*, *209*, 1516–1534.

Tytell, E. D., Standen, E. M., & Lauder, G. V. (2007). Escaping Flatland: Three-dimensional kinematics and hydrodynamics of median fins in fishes. *Journal of Experimental Biology*, *211*, 187–195.

Webb, P. W., & Keyes, R. S. (1981). Division of labor between median fins in swimming dolphin (Pisces: Coryphaenidae). *Copeia*, *1981*, 901–904.

Yates, G. T. (1983). Hydromechanics of body and caudal fin propulsion. In P. W. Webb & D. Weihs (Eds.), *Fish biomechanics* (pp. 177–213). New York: Praeger.

SUPPORTING INFORMATION

Additional Supporting Information may be found online in the supporting information tab for this article.

How to cite this article: Weickhardt AF, Feilich KL, Lauder GV. Structure of supporting elements in the dorsal fin of percid fishes. *Journal of Morphology*. 2017;00:1–10. https://doi.org/10.1002/jmor.20744

SGML and CITI Use Only
DO NOT PRINT

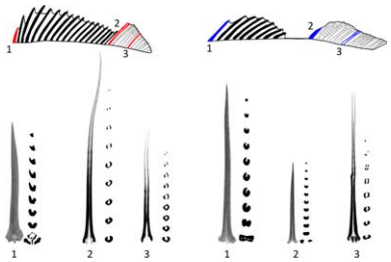

In fishes the dorsal fin can be a single contiguous structure (red) or it may be separated (blue) into an anterior, spiny dorsal fin and a posterior, soft dorsal fin. We hypothesized that fishes with separated dorsal fins would have stiffened fin elements at the leading edge of the soft dorsal fin in order to resist hydrodynamic loading during swimming. Our micro-CT-data showed no significant difference in cross-sectional shape or size between the leading edge of the soft dorsal fin in fishes with separated fins and the equivalent fin element in fishes with contiguous fins.